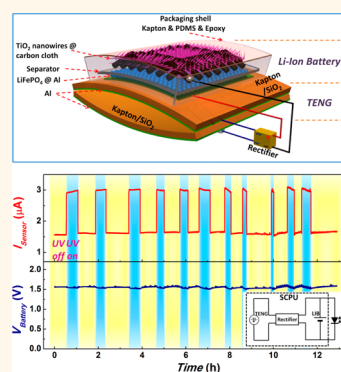


Motion Charged Battery as Sustainable Flexible-Power-Unit

Sihong Wang,[†] Zong-Hong Lin,[†] Simiao Niu,[†] Long Lin,[†] Yannan Xie,[†] Ken C. Pradel,[†] and Zhong Lin Wang^{†,*,‡}

[†]School of Materials Science and Engineering, Georgia Institute of Technology, Atlanta, Georgia 30332-0245, United States and [‡]Beijing Institute of Nanoenergy and Nanosystems, Chinese Academy of Sciences, Beijing 100083, China

ABSTRACT Energy harvesting and storage are the two most important energy technologies developed for portable, sustainable, and self-sufficient power sources for mobile electronic systems. However, both have limitations for providing stable direct-current (DC) with an infinite lifetime. Herein, we integrated a triboelectric nanogenerator (TENG)-based mechanical energy harvester with Li-ion-battery (LIB)-based energy storage as a single device for demonstrating a flexible self-charging power unit (SCPU), which allows a battery to be charged directly by ambient mechanical motion. This physical integration enables a new operation mode of the SCPU: the “sustainable mode”, in which the LIB stores the TENG-generated electricity while it is driving an external load. With the LIB being replenished by the ambient mechanical energy, the SCPU can keep providing a constant voltage to the load by utilizing the stable difference between the battery's intrinsic electrode potentials. This study will impact the traditional trends of battery research and advance the development of the self-powered systems.



KEYWORDS: mechanical energy harvesting · energy storage · triboelectric nanogenerator · lithium ion battery · self-powered system

The emergence of electronic devices and systems^{1–3} with unprecedented functionalities and advanced human-machine interfacing mandatorily requires portable, lightweight, and possibly sustainable power sources. Unlike the large-scale power source that is mostly characterized by cost, such power sources for mobile electronics are characterized by availability, stability, and efficiency.⁴ Energy generation^{4–9} and storage^{9–12} are the two most important areas for developing new power sources, and they are usually two separated units based on two consecutive processes, which have limitations as sustainable power sources. Targeting at the self-powered systems^{13,14} that have a high mobility, excellent working-condition adaptability and stability, energy generators that function by harvesting energy from the working/living environmental usually have uncontrollable fluctuation/instability in their outputs that are greatly influenced by the change in ambient environment. Take the mechanical energy harvesting as an example, although the recently invented triboelectric nanogenerator (TENG) is proven to be a powerful and promising technology that is highly efficient, low-cost, and environmentally friendly,^{15–21} the electricity generated consists of noncontinuous pulses with irregular

magnitude; thus, it cannot be directly used to drive most electronic devices that need a constant DC voltage supply. Energy storage devices such as batteries,^{10,22–25} on the other hand, can provide a constant voltage at their discharging plateau to act as the direct power sources for most portable and wireless electronic devices. But the intrinsic problem of batteries is the limited lifetime, so that they have to be charged or replaced periodically; otherwise, batteries can be “deadly drained”.

To develop sustainable power sources by complementarily combining the advantages of these two technologies²⁶ as presented above, here we demonstrate the first flexible self-charging power unit (SCPU) that is capable of simultaneously harvesting and storing ambient mechanical energy, by integrating a TENG-based mechanical energy harvester and a Li-ion battery (LIB) based energy storage. In this SCPU, the Li-ion battery portion can be directly charged by mechanical motions. The integration was realized through developing a flexible LIB on an arch-shaped TENG structure.¹⁶ When the surrounding mechanical energy is applied onto the SCPU, an alternating current in response to the external triggering is generated. After rectification, the electrical energy can be stored in the LIB, which can be fully charged in 11 h. With this

* Address correspondence to zlwang@gatech.edu.

Received for review September 27, 2013 and accepted November 19, 2013.

Published online November 23, 2013
10.1021/nn4050408

© 2013 American Chemical Society

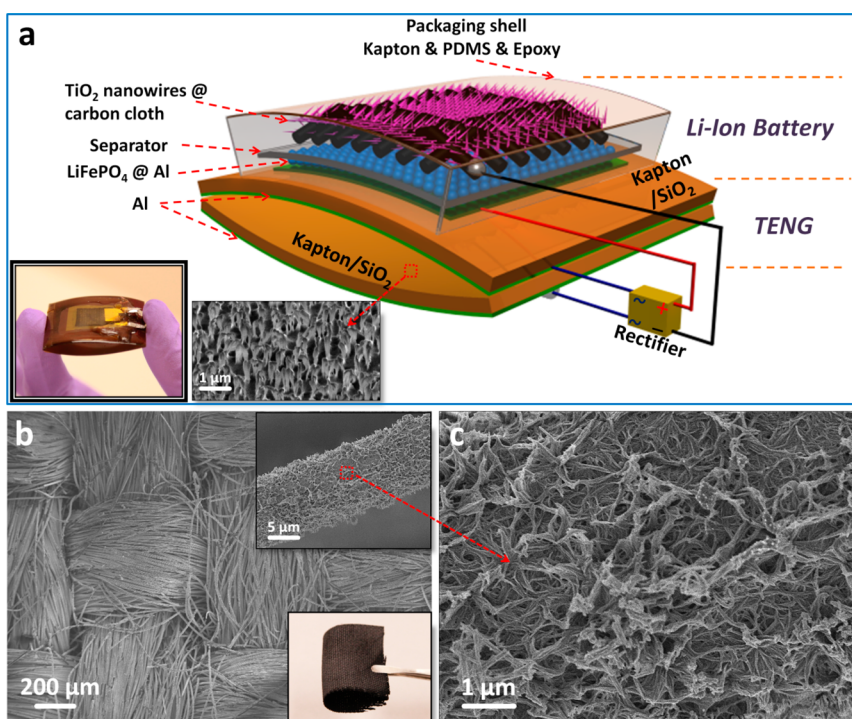


Figure 1. Structure design of a flexible self-charging power unit (SCPU). (a) Schematic diagram showing the detailed structure of the SCPU, the inset on the left is a photograph of a typical SCPU device, and the inset on the right is an SEM image of the Kapton nanorod-structure on the concave surface of the bottom Kapton, with 30°-tilted view. (b) SEM image of the carbon cloth grown with TiO₂ nanowire (NW) networks, the top inset is the enlarged SEM image of a single fiber in the fabric, and the bottom inset is a photograph of the TiO₂-covered carbon cloth as the anode, showing its good flexibility. (c) SEM image with higher magnification showing the detailed morphology of the TiO₂ NW networks on the carbon cloth.

SCPU, we demonstrated a new working mode for a power source, the “sustainable mode”, in which the environmental mechanical energy is scavenged to charge the battery while the battery keeps driving an external load as a DC source. In this mode, the demonstrated SCPU can provide a continuous and sustainable DC current of 2 μ A at a stable voltage of 1.55 V for as long as there is mechanical motion/agitation. It can be used to continuously drive a UV sensor²⁷ for extended period of time. The LIB in the SCPU serves not only as energy storage, but also as a power regulator and management for the entire system by utilizing the stable electrode-potential difference.^{10,28} Since mechanical motion is available almost everywhere and at any time to replenish the energy draining in the battery, a large-capacity battery with a high density may not be necessary to ensure a long operating lifetime. This could introduce a new alternative to the current research trend of solely seeking high density batteries. Our study demonstrates a self-charging, self-sufficient, sustainable, flexible, and potentially maintenance-free mobile power source that can be used for powering personal electronics, medical devices, and environmental/infrastructure sensors.

RESULTS AND DISCUSSION

The integration of a LIB and a TENG in the SCPU was achieved through the construction of a flexible LIB, which was made in an arch shape for creating the gap

necessary for the TENG structure,¹⁸ as illustrated in Figure 1a. To make the battery flexible, we designed a polymeric shell for the packaging and sealing, to replace the conventional ridge coin cell. The supporting substrate of this polymeric shell is a bent Kapton film (3 cm \times 4 cm) with purposely introduced thermal stress through the deposition of a SiO₂ film at high temperature.^{18,29} The three kernel components of the LIB, the TiO₂ nanowires (NWs)^{30,31} anode, the polyethylene (PE) separator, and the LiFePO₄/active carbon/binder mixture cathode on the Al current collector, were laminated on top of the convex surface (the surface deposited with SiO₂) of this Kapton substrate. This kernel structure with an effective area of \sim 1.5 cm \times 1.5 cm was immersed in the electrolyte. To enhance the flexibility of the battery from the anode side, the TiO₂ NWs with an anatase crystal structure (Figure S1) were hydrothermally grown on a piece of soft carbon cloth that also serves as the current collector,³² as shown by the scanning electron microscopy (SEM) image displayed in Figure 1b. From the picture of the TiO₂/carbon cloth composite shown in the inset (bottom) of Figure 1b, this anode layer exhibits excellent flexibility. SEM images with higher magnifications are shown at the top inset of Figure 1b (the morphology of a single fiber from the carbon cloth after the growth of TiO₂ nanowire networks), and Figure 1c, from which we can tell that every single fiber in the carbon cloth is uniformly covered by TiO₂ NW networks

with an average length of $\sim 1 \mu\text{m}$. As a comparison, the SEM image of the carbon cloth before the growth of TiO_2 NW networks is shown in Figure S2. The battery was isolated from air by covering with a layer of thin Kapton film and sealing with polydimethylsiloxane (PDMS) and epoxy at the sides. For the hybridization with the TENG, this LIB's supporting Kapton substrate was deposited with Al film on the back and bonded with another bent Kapton film of the same size in a face-to-face manner. This forms an arch-shaped TENG structure based on the triboelectrification between the top Al layer and the bottom Kapton that has the corresponding electrode (Al film) deposited on its convex surface. To enhance the triboelectric charge density through large surface roughness and increased effective contact area,^{16,17} the concave surface of the bottom Kapton was pretreated with inductive coupling plasma (ICP) reactive ion etching, to produce the nanorod-covered surface,³³ as shown in the inset (right) of Figure 1a. With this hybridized SCPU structure, the LIB can be charged through harnessing ambient mechanical energy, only by rectifying the TENG-generated alternating-current (AC) pulses to DC with a full-wave bridge rectifier. A photo of a typical SCPU device is shown in the inset (left) of Figure 1a, clearly revealing its flexibility and arch-shaped structure. The detailed fabrication process of the SCPU is described in the Methods session.

When external mechanical vibration is applied onto the flexible SCPU to periodically flatten it, the two surfaces across the gap will get into contact from time to time. Coupling of the triboelectric effect with the electrostatic induction will generate a flow of current in the external circuit, which will be stored in the LIB in the same device. We now illustrate the simultaneous charge generation and storage process of the SCPU without connecting to an external load. The basic working principle can be divided into several stages, as shown in Figure 2 (for clarity, the arch-shaped SCPU is depicted as a flat structure and the periodic change of the gap is expressed as the change of spacing between the two parts). In its starting state (Figure 2a) before any mechanical deformations to induce the contact between the two surfaces, there are no triboelectric charges (tribo-charges) and thus no current generation. When the ambient mechanical vibration applies a pressing force onto the SCPU, the structure will be flattened, so that the top Al and bottom Kapton across the gap will be brought into contact (Figure 2b). Due to the triboelectric effect,^{34,35} the electrons will transfer from the Al to the Kapton because of the difference in electron attractions.³⁶ This will produce positive tribo-charges on the Al surface while the Kapton surface will develop negative charges of the same density. At this very moment, there is no induced electrical potential to drive the flow of current; thus, the LIB is not being charged. Once the pressing force is withdrawn (Figure 2c), the SCPU will start to return to its original arch shape immediately, separating the opposite

tribo-charges. This will induce a higher potential in the top Al layer, which will drive the flow of current from the top Al to the bottom electrode, and through the LIB from its positive electrode to its negative electrode as a result of the full-bridge rectification. The charging reactions at the two electrodes are enabled by this current, which stores the generated electrical energy. This will last until the SCPU fully returns to its original shape and the accumulation of the transferred charges completely screens the tribo-charge-induced potential (Figure 2d). Ideally, the amount of charges stored in the LIB during this half cycle should equal to the number of tribo-charges on the Kapton surface. Subsequently, once the SCPU is pressed again (Figure 2e), the distance between the opposite tribo-charges will be reduced, so that the induced potential difference between the two electrodes will begin to diminish. The transferred charges will flow back to re-establish the equilibrium, which will contribute to the second current peak through the rectifier in the reverse direction. Because of the rectifier, the current through the LIB will still be in the charging direction so that the electrical energy in this second half cycle will be stored until the SCPU reaches the state in Figure 2b again. When the SCPU is subjected to a lasting mechanical agitation, this cycle from Figure 2b to 2e will keep taking place so that more and more energy will be stored in the LIB part of the SCPU.

The SCPU when it is being simultaneously charged and discharged due to the connection to an external load is shown in Figure 2f. The AC pulses generated by the TENG are first rectified, and then directed into the LIB from its positive electrode. But when the LIB is connected to the external load, the positive electrode is always at a higher potential. This causes the current to flow from the positive electrode to the load, which will be in the reversed direction in reference to the charging current, but flowing through two separated electrical connections. Thus, the electrochemical reactions corresponding to both charging and discharging are occurring simultaneously at each electrode. The voltage applied across the load will be the voltage of the LIB (Figure 2f), which is determined by the difference in the electrode potentials of the two half-reactions. Since the electrode potential is not affected by the state of charge (SOC) within the wide-range discharging plateau,^{10,28} the irregular and fluctuating current generated by the TENG due to the change of the surround mechanical motion will not cause an obvious change in the output voltage of the LIB. This stable constant voltage on the load should be able to be maintained for an infinitely long time in principle, as long as the averaged current provided by the TENG over time is about the same as the current consumed by the load, so that the SOC of the LIB does not shift out of the voltage plateau. In this proposed integration mode of mechanical energy harvesting and energy storage, the consumed energy is generated from the

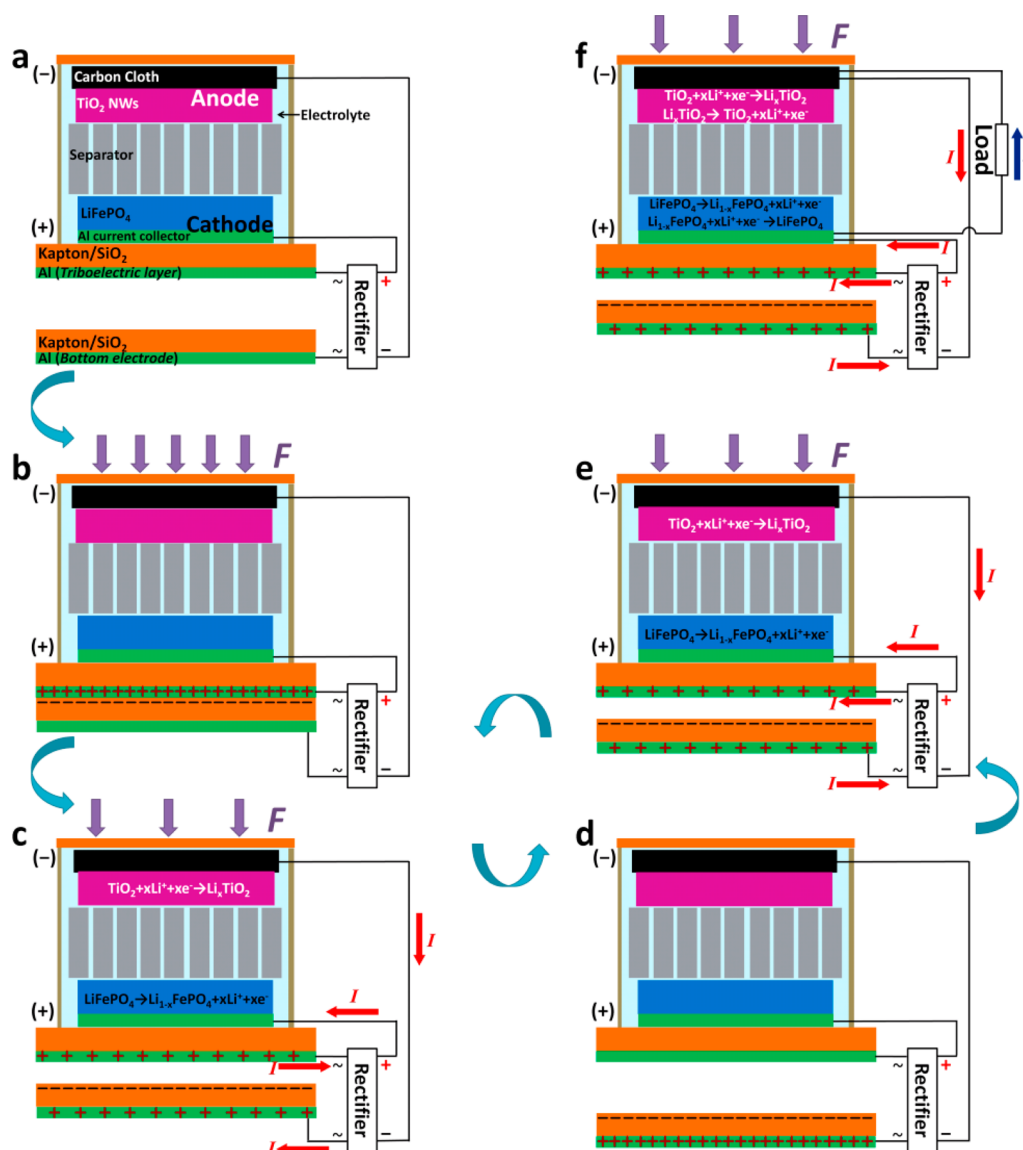


Figure 2. Basic working principle of the SCPU. (a) A two-dimensional sketch showing the structure and the original state of the SCPU before mechanical deformation. For clarity, the arch-shape is expressed as a flat structure. (b) Mechanical pressing brings the top Al and the bottom Kapton into contact, generating opposite triboelectric charges on the two surfaces. (c) The force is releasing and the SCPU is reverting to its original arch shape. The induced potential difference generates the first current peak, which charges the LIB part. (d) The SCPU returns to its original shape, with induced potential difference fully screened. (e) The SCPU is pressed again and the redundant charges on the bottom electrodes flows back, generating the second current peak to charge the LIB part. (f) A new operation mode, in which the LIB part is driving an external load while being charged by the TENG part. Both the charging and discharging reactions take place at the electrodes (the blue arrow stands for the discharging current through the load).

surrounding mechanical motion; thus, the amount of energy stored in the LIB will not change very much although the load is being driven continuously. Therefore, the battery works not only as an energy storage unit, but more importantly as a power regulator that converts the irregular, unstable and time-dependent input from the TENG (due to the varying ambient condition), to a constant DC output. This is the reason that the SCPU can be a stable DC power source.

The performance of the SCPU is first characterized by the outputs of the TENG and the LIB as individual units (Figure 3). When the arch-shaped structure was periodically flattened under a frequency of 8 Hz, an

open-circuit voltage (V_{OC}) of ~ 220 V was generated between the two electrodes of the TENG part (Figure 3a), which is the potential difference induced by the separation of opposite tribo-charges on the Al and Kapton films. Under a short-circuit condition, this voltage drives ~ 110 nC of charges (ΔQ) to flow between the two electrodes in each half deformation cycle (as shown in the measured charge transfer in Figure 3b). This value should theoretically equal to the amount of tribo-charges on each triboelectric surface (with an area of ~ 12 cm²), corresponding to a charge density of ~ 91.6 $\mu\text{C}/\text{m}^2$. This back-and-forth charge transfer produced a pair of AC short-circuit current (I_{SC})

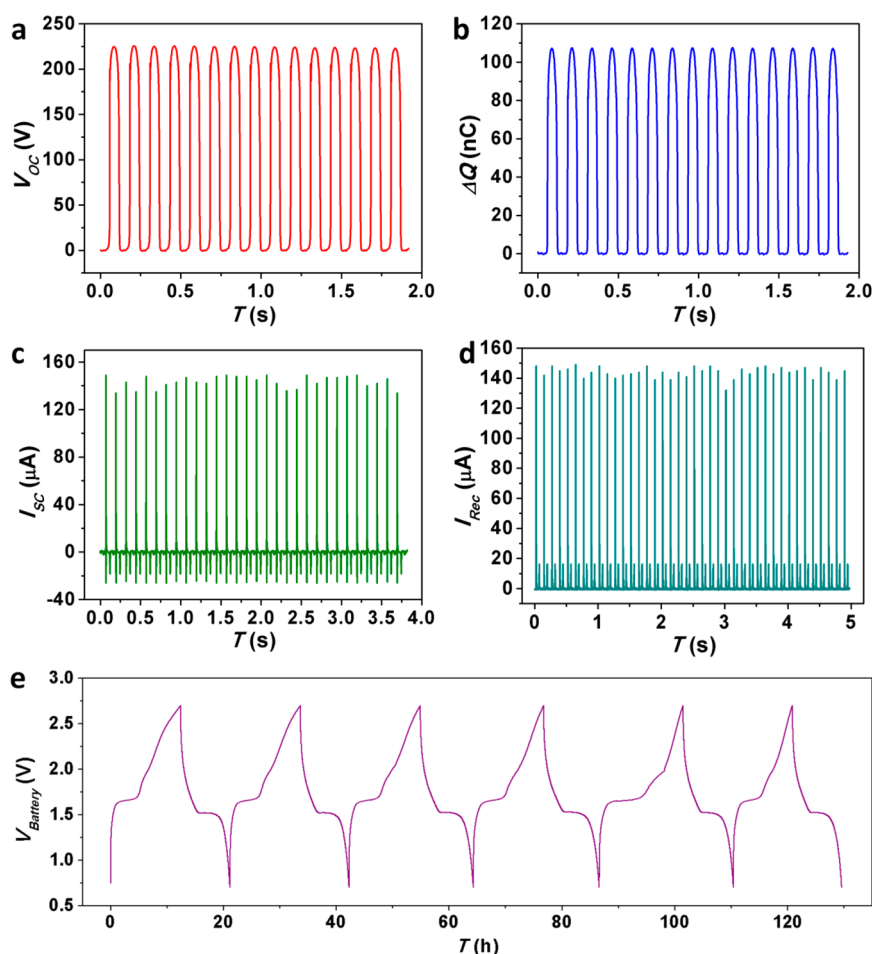


Figure 3. Characterizing the individual performances of the TENG part and the LIB part in the SCPU. (a) The open-circuit voltage (V_{OC}), (b) the amount of charges transferred (ΔQ), (c) the short-circuit current (I_{SC}) and (d) the rectified current (I_{Rec}) generated by the TENG part when the SCPU is periodically flattened by external mechanical agitation under the frequency of 8 Hz. (e) The voltage profile of the LIB part during the deep charging/discharging galvanostatic test with a current of $2 \mu\text{A}$.

peaks in each cycle. As shown in Figure 3c, the positive peak with a larger magnitude of $\sim 150 \mu\text{A}$ came from the pressing motion, which had a higher deformation rate compared to the elastic releasing process. But these two asymmetric peaks per cycle carry the same amount of charges due to charge conservation (Figure 3b). This AC output can be rectified to DC by a low-loss full wave bridge rectifier (Figure 3d), which generates $\sim 220 \text{ nC}$ electricity per cycle to be stored in the LIB. The performance of the arch-shaped TENG part was also tested under nonperiodic deformations by applying force with our hand, with the measured V_{OC} and ΔQ shown in Figure S3. We find that the electricity generation of the TENG part is not affected by the variation in the deformation frequency.

The capability of the flexible LIB in the SCPU for charge storage was evaluated using deep charging/discharging galvanostatic test between 0.7 and 2.7 V, at a current of $2 \mu\text{A}$, as for conventional batteries. As indicated by the voltage profile in the 6 consecutive cycles (Figure 3e), the LIB gave clear voltage plateaus in both charging and discharging processes. The discharging

plateau is $\sim 1.53 \text{ V}$, which is the real working voltage of the LIB as a power source. The LIB also has a stable capacity around $17.5 \mu\text{Ah}$ (Figure S4), revealing its expected performance as an energy storage unit.

When the TENG part and the LIB part work conjunctively as a full unit, the SCPU will work as a self-sufficient power source. Conventionally, the charging and discharging of an energy storage unit is in two separated and consecutive steps. This working mode for the SCPU is called the “standby-active mode”,¹⁴ as shown schematically in the circuit diagrams in Figure 4a. The LIB is connected to the TENG through the rectifier but disconnected from the load (with S1 closed and S2 open), during which it is only storing the electrical energy generated by the TENG part. As demonstrated in Figure 4b, the LIB was charged to its full capacity in $\sim 11 \text{ h}$ by the TENG under a deformation frequency of 9 Hz, with the voltage (V_{Battery}) increasing from 0.7 to 2.5 V crossing the charging plateau at $\sim 1.62 \text{ V}$. This is the “standby mode” during which the SCPU is charged. Next, the fully charged SCPU will be used as a battery to drive a device by switching the

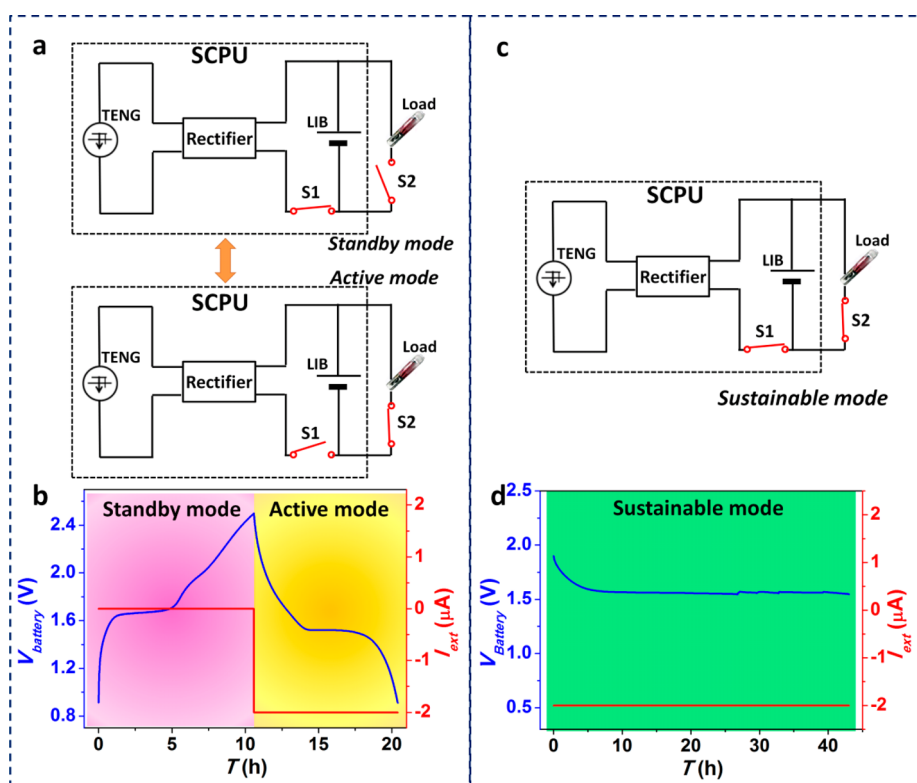


Figure 4. Performance of the SCPU as an integrated DC power source. (a) Electrical circuit diagram showing the “standby-active mode” for the integration of the TENG part and the LIB part. The portion enclosed by the dotted square is the SCPU. (b) The voltage profile showing the LIB part fully charged by the TENG part (the “standby mode”) and then discharging under a current of 2 μA (the “active mode”). (c) The electrical circuit diagram showing the newly proposed “sustainable mode”, in which the LIB part is driving the external load while it is being charged by the TENG part. (d) In this sustainable mode, the SCPU provided a 2- μA DC current with a constant voltage of 1.53 V for more than 40 h, when the SCPU was deformed under a frequency of 9 Hz.

connection with S1 open and S2 closed. As shown in Figure 4b, the fully charged LIB could provide a constant current of 2 μA to the external load for ~ 10 h (~ 3 h at the discharging plateau, which is the actual working time for this LIB as a constant-voltage power source). This is the “active mode” of the SCPU during which it is used to drive a device. In practical applications, the SCPU switches between the “standby mode” and the “active mode”, which correspond to the charging and discharging of the LIB, respectively. This operational integration methodology of energy harvesting and storage is particularly suitable for applications where the current required by certain electronic devices is much larger than the average current (rather than the peak current) generated by the TENG, and the electronic devices do not need to work continuously. This meets the requirement of some sensors for intermittent detections.

Alternatively, in the cases that the electronic devices need to work constantly, the SCPU can work in a “sustainable mode”, as proposed in Figure 4c. In this mode, the LIB is being charged by the TENG while it is simultaneously powering an external load. As long as the averaged current converted from the surrounding mechanical energy is approximately the same as the

current required by the load, the energy stored in the LIB will remain at a stable level so that the voltage can remain at its discharging plateau “forever” due to the nature of electrochemical reactions (as discussed in Figure 2f). As shown in Figure 4d, when the SCPU was being triggered by a pressing motion at 9 Hz (the averaged current produced can be estimated as $\sim 1.98 \mu\text{A}$ according to the result of the measured charge transfer in Figure 2b), the LIB part provided a constant current of 2 μA at the voltage of ~ 1.55 V for more than 40 h! Thus, in this proposed “sustainable mode”, the SCPU could work as an independent, self-sufficient and sustainable power source for providing a constant voltage.

In a lot of applications, a constant voltage from the power source is needed for the operation of the electronic systems. For example, in a sensing system for detecting the change in the environment through the resulted change of the sensor's effective resistance, the current as the measurable signal should solely depend on the sensor's resistance, so that the whole system can be calibrated. For many sensing purposes, changes in the environment need to be constantly monitored without interruption so that any undesired instances can be detected immediately; thus, the use

of battery may have its limitation due to its relatively short lifetime. The demonstrated SCPU under the “sustainable mode” can serve as a nonstop power source for these applications. We used a ZnO-nanowire-based UV sensor²⁷ to demonstrate this unique capability of the SCPU. In the sensor, the nanowire is bonded onto the substrate at its two ends with silver paste, forming a metal-semiconductor-metal structure (the left inset of Figure 5a). A Schottky contact is formed so that the I–V has a rectifying behavior (Figure S5). In the first case (Figure 5a), we only used the fully charged LIB portion of the SCPU to power this UV sensor as shown in the inset (right) of Figure 5a, which is the “active mode” of the SCPU illustrated in Figure 4a. When the UV light was off, with an input voltage of ~ 1.53 V from the battery at its discharging plateau, the measured current through the sensor was around $1.55 \mu\text{A}$. When UV light was turned on, the current jumped to a level of $\sim 2.95 \mu\text{A}$. We periodically turned the UV light on and off, and the voltage of the battery remained stable during the first few cycles. However, after ~ 3.5 h, the voltage started to drop, which indicated that the battery was running out of charge. As a result, the current levels for the UV-off and UV-on states both decreased to lower levels, and thus could not be an effective indicator for the presence of UV-illumination anymore since it cannot be judged using the calibrated current, which means that this battery has to be replaced after about 4 h usage.

This problem can be solved using the SCPU in the proposed “sustainable mode”. As shown in Figure 5b, when the LIB was being charged by the TENG under a deformation frequency of 9 Hz while driving the UV sensor, the output voltage of the battery can stay at the plateau of around 1.55 V with only small fluctuation for over 12 h, during which the UV light was periodically turned on and off for more than 10 times without obvious decay in current level, which can clearly convey the information of the UV illumination to the calibrated system. Therefore, it has been undoubtedly demonstrated that with the “hybridization” of the mechanical energy harvesting and energy storage in the SCPU, an electronic system could be truly self-powered continuously and sustainably.

Through integrating the mechanical energy harvesting and the energy storage both physically and operationally, the intrinsic limitations of these two technologies can be remarkably overcome. For the electricity generated by TENGs, the electrical output is pulse-shaped^{17,18,21} due to their fundamental working mechanism. This output is often noncontinuous and irregular, therefore cannot be used to directly power electronic devices in most cases. By combining a TENG with a LIB in the “sustainable mode”, the TENG's only function is to replenish the energy drain in the LIB, so that the harvested mechanical energy can be used to drive the load at a constant voltage through the LIB,

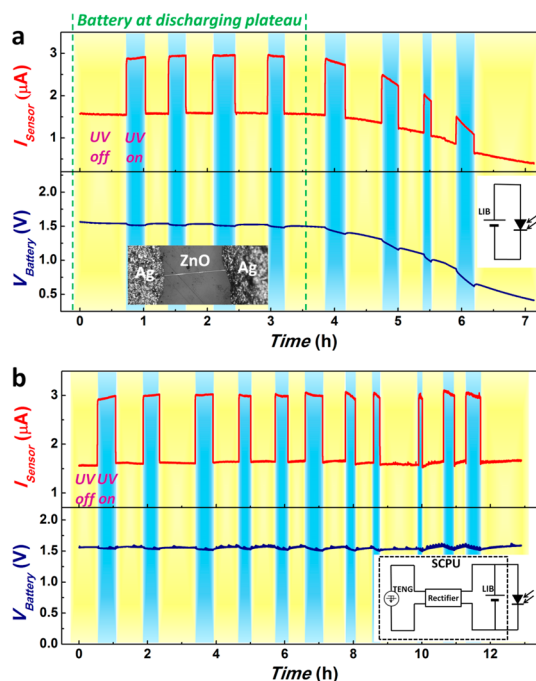


Figure 5. The SCPU as a sustainable power source for driving a UV sensor. (a) Operation of the UV sensor when solely driven by the LIB part of the SCPU, which was recorded from the point that the battery just entered its discharging plateau. The left inset is an optical microscope image of the ZnO-nanowire-based UV sensor in this demonstration, and the right inset is the circuit diagram showing the power source. (b) The operation of the UV sensor continuously driven by the SCPU in the “sustainable mode” for ~ 13 h. The inset is the circuit diagram showing the UV sensor powered by the SCPU in the “sustainable mode”. In both of (a) and (b), the top curve (red) is the current through the sensor, reflecting its response to the UV light, and the bottom curve (blue) is the real time voltage of LIB part.

which benefits from the stable potential difference between the two electrodes in the electrochemical reaction. Thus, in this integration, the battery works not only as an energy storage, but also as a power regulator (for changing the pulsed electrical outputs into a constant voltage), not just as an energy storage unit. This is a new role for batteries, and can potentially change the traditional views in the battery technology. Since the stored energy in the battery will not be fully used up, having a large capacity in the battery for a longer lifetime through the improvement of the materials' energy densities is no longer essential, which, however, is the current trend in battery research. Also, the size and weight of the battery can be miniaturized, and waste chemicals from dead batteries can be greatly reduced. Moreover, this demonstration opens the door to a new research field for developing long lifetime power sources, that is a wise integration of the TENG and the battery, in the aspects such as the appropriate design of the TENG to meet the desired energy consumption of the load, the optimum capacity of the battery to tolerate the estimated output fluctuation of the TENG in certain environment, and so on.

CONCLUSIONS

In summary, through building a flexible Li-ion battery (LIB) on an arch-shaped structure, we have developed a self-charging power unit (SCPU) that integrates the triboelectric-effect-based mechanical energy harvester and electrochemical energy storage into one device. As triggered by ambient mechanical vibrations, the TENG part can efficiently generate electricity with high output, and the rectified electrical energy can be stored in the LIB part. Besides the conventional “stand-by-active mode” for the operation of the SCPU as an integrated power source, we proposed a new mode for the integration, the “sustainable mode”, in which the surrounding mechanical energy is harvested and simultaneously stored in the LIB, while the LIB is driving an external device. In the experimental demonstration,

the SCPU in this mode can provide a constant voltage with a DC current of $2\ \mu\text{A}$ for over 40 h (compared to 3.5 h for the LIB alone), and is capable of continuously powering the operation of a UV sensor at a constant voltage. Hence, the integrated power sources developed from the concept of the SCPU in the proposed “sustainable mode” can potentially serve as an independent, portable, sustainable, and stable power unit, which will meet the general requirement of almost any electronic device and make the self-powered system more feasible by harvesting ambient mechanical energy. Additionally, the hybridization of these two types of energy devices into a single unit helps to achieve a compact, lightweight, and multifunctional power source, with improved portability. Our study provides a breakthrough progress in mobile energy and will have a profound influence on the future technology.

METHODS

Growth of the TiO₂ Nanowire Networks on the Carbon Cloth. The carbon cloth was first ultrasonically cleaned in acetone, ethanol, and DI water for 30 min each, and then placed in a 50-mL Teflon-lined stainless steel autoclave. Next, 1 g of TiO₂ (P25) powder and 40 mL of NaOH (10 M) were added into the autoclave and the solution was mixed with the carbon cloth for another 30 min. After it was sealed, the autoclave was kept in an oven at 200 °C for 12 h, and then cooled down in air. After this first-step hydrothermal reaction, the carbon cloth covered with Na-titanate nanowire networks was washed with water and immersed in HCl solutions (1 M, 40 mL) for 10 min to replace Na⁺ with H⁺, forming H-titanate nanowire networks. After that, this piece of carbon cloth was washed with water again, and then dried at ambient temperature. After the sample was heat-treated at 500 °C for 3 h under Ar atmosphere, TiO₂ nanowire networks on the carbon cloth were obtained.

Fabrication of the Flexible Self-Charging Power Unit (SCPU). The fabrication process of SCPU starts from making the bent Kapton substrate. After they were ultrasonically cleaned in acetone, menthol, and DI water consecutively, the Kapton films (125- μm thick) with the size of 3 cm \times 4 cm were deposited with a layer of SiO₂ film with a thickness of 500 nm at 250 °C using the plasma-enhanced chemical vapor deposition (PECVD). Upon cooling down, the Kapton substrates automatically bent toward the SiO₂ side. Then, those Kapton substrates were divided into two groups (named as Kapton 1 and Kapton 2) for different fabrication processes. Kapton 1 was deposited with 100-nm Al on its concave surface using the e-beam evaporator. Then, on the convex surface of this Kapton, we stacked three layers in the following order: TiO₂-nanowire-covered carbon cloth (1.5 cm \times 1.5 cm) as the anode, PE separator (2 cm \times 2 cm), the LiFePO₄/active-carbon/binder mixture on Al foil (1.5 cm \times 1.5 cm) as the cathode (the anode and the cathode were connected with leads before this step). Then, they were fully covered by a piece of thin Kapton film (with dimensions of 2.5 cm \times 2.5 cm \times 2.5 μm) on top. Three sides of the top Kapton were sealed with the bottom Kapton substrate using the PDMS, forming a shell with one side open. Then, the whole structure was transferred into the oven with the temperature of 120 °C, to cure the PDMS and dry the structure. After baking for 12 h, this part was put into a glovebox filled with Ar. The electrolyte (1 M LiPF₆ in 1:1:1 ethylene carbonate/dimethyl carbonate/diethyl carbonate) was injected into the shell through the open side. Finally, this side was sealed with epoxy, leaving the two leads extending outward. This gave us a flexible LIB on the bent Kapton 1. For Kapton 2, the concave surface was sputtered with a 10-nm Au thin film as the mask and then etched by inductively coupled plasma (ICP) reactive ion etching for creating the nanorod-structure. On the other side of

this Kapton 2, a layer of 100-nm Al was deposited as the bottom electrode. In the end, by bonding the Kapton 1 and Kapton 2 at the two ends, we got the arch-shaped SCPU.

Conflict of Interest: The authors declare no competing financial interest.

Supporting Information Available: More detailed information about the crystalline structure of the TiO₂ nanowire network on the carbon cloth, the discharging capacity of the LIB part in the SCPU, and the I–V curves of the ZnO-NW-based UV sensor. This material is available free of charge via the Internet at <http://pubs.acs.org>.

Acknowledgment. Research was supported by Airforce, U.S. Department of Energy, Office of Basic Energy Sciences under Award DEFG02-07ER46394 and the Knowledge Innovation Program of the Chinese Academy of Sciences (Grant KJCX2-YW-M13).

REFERENCES AND NOTES

- Tian, B. Z.; Cohen-Karni, T.; Qing, Q.; Duan, X. J.; Xie, P.; Lieber, C. M. Three-Dimensional, Flexible Nanoscale Field-Effect Transistors as Localized Bioprobes. *Science* **2010**, *329*, 830–834.
- Kim, D. H.; Lu, N. S.; Ma, R.; Kim, Y. S.; Kim, R. H.; Wang, S. D.; Wu, J.; Won, S. M.; Tao, H.; Islam, A.; *et al.* Epidermal Electronics. *Science* **2011**, *333*, 838–843.
- Wu, W. Z.; Wen, X. N.; Wang, Z. L. Taxel-Addressable Matrix of Vertical-Nanowire Piezotronic Transistors for Active and Adaptive Tactile Imaging. *Science* **2013**, *340*, 952–957.
- Wang, Z. L.; Zhu, G.; Yang, Y.; Wang, S. H.; Pan, C. F. Progress in Nanogenerators for Portable Electronics. *Mater. Today* **2012**, *15*, 532–543.
- Oregan, B.; Gratzel, M. A Low-Cost, High-Efficiency Solar-Cell Based on Dye-Sensitized Colloidal TiO₂ Films. *Nature* **1991**, *353*, 737–740.
- Law, M.; Greene, L. E.; Johnson, J. C.; Saykally, R.; Yang, P. D. Nanowire Dye-Sensitized Solar Cells. *Nat. Mater.* **2005**, *4*, 455–459.
- Dresselhaus, M. S.; Chen, G.; Tang, M. Y.; Yang, R. G.; Lee, H.; Wang, D. Z.; Ren, Z. F.; Fleurial, J. P.; Gogna, P. New Directions for Low-Dimensional Thermoelectric Materials. *Adv. Mater.* **2007**, *19*, 1043–1053.
- Wang, Z. L.; Song, J. H. Piezoelectric Nanogenerators Based on Zinc Oxide Nanowire Arrays. *Science* **2006**, *312*, 242–246.
- Arico, A. S.; Bruce, P.; Scrosati, B.; Tarascon, J. M.; Van Schalkwijk, W. Nanostructured Materials for Advanced Energy Conversion and Storage Devices. *Nat. Mater.* **2005**, *4*, 366–377.

10. Tarascon, J. M.; Armand, M. Issues and Challenges Facing Rechargeable Lithium Batteries. *Nature* **2001**, *414*, 359–367.
11. Poizot, P.; Laruelle, S.; Grugeon, S.; Dupont, L.; Tarascon, J. M. Nano-Sized Transition-Metal Oxides as Negative-Electrode Materials for Lithium-Ion Batteries. *Nature* **2000**, *407*, 496–499.
12. Simon, P.; Gogotsi, Y. Materials for Electrochemical Capacitors. *Nat. Mater.* **2008**, *7*, 845–854.
13. Wang, Z. L. Self-Powered Nanosensors and Nanosystems. *Adv. Mater.* **2012**, *24*, 280–285.
14. Hu, Y. F.; Zhang, Y.; Xu, C.; Lin, L.; Snyder, R. L.; Wang, Z. L. Self-Powered System with Wireless Data Transmission. *Nano Lett.* **2011**, *11*, 2572–2577.
15. Fan, F. R.; Tian, Z. Q.; Wang, Z. L. Flexible Triboelectric Generator!. *Nano Energy* **2012**, *1*, 328–334.
16. Fan, F. R.; Lin, L.; Zhu, G.; Wu, W. Z.; Zhang, R.; Wang, Z. L. Transparent Triboelectric Nanogenerators and Self-Powered Pressure Sensors Based on Micropatterned Plastic Films. *Nano Lett.* **2012**, *12*, 3109–3114.
17. Zhu, G.; Pan, C. F.; Guo, W. X.; Chen, C. –Y.; Zhou, Y. S.; Yu, R. M.; Wang, Z. L. Triboelectric-Generator-Driven Pulse Electrodeposition for Micropatterning. *Nano Lett.* **2012**, *12*, 4960–4965.
18. Wang, S. H.; Lin, L.; Wang, Z. L. Nanoscale Triboelectric-Effect-Enabled Energy Conversion for Sustainably Powering Portable Electronics. *Nano Lett.* **2012**, *12*, 6339–6346.
19. Zhu, G.; Lin, Z.-H.; Jing, Q. S.; Bai, P.; Pan, C. F.; Yang, Y.; Zhou, Y. S.; Wang, Z. L. Toward Large-Scale Energy Harvesting by a Nanoparticle-Enhanced Triboelectric Nanogenerator. *Nano Lett.* **2013**, *13*, 847–853.
20. Zhang, X. S.; Han, M. D.; Wang, R. X.; Zhu, F. Y.; Li, Z. H.; Wang, W.; Zhang, H. X. Frequency-Multiplication High-Output Triboelectric Nanogenerator for Sustainably Powering Biomedical Microsystems. *Nano Lett.* **2013**, *13*, 1168–1172.
21. Wang, S. H.; Lin, L.; Xie, Y. N.; Jing, Q. S.; Niu, S. M.; Wang, Z. L. Sliding-Triboelectric Nanogenerators Based on In-Plane Charge-Separation Mechanism. *Nano Lett.* **2013**, *13*, 2226–2233.
22. Chan, C. K.; Peng, H. L.; Liu, G.; McIlwrath, K.; Zhang, X. F.; Huggins, R. A.; Cui, Y. High-Performance Lithium Battery Anodes Using Silicon Nanowires. *Nat. Nanotechnol.* **2008**, *3*, 31–35.
23. Kang, B.; Ceder, G. Battery Materials for Ultrafast Charging and Discharging. *Nature* **2009**, *458*, 190–193.
24. Kovalenko, I.; Zdyrko, B.; Magasinski, A.; Hertzberg, B.; Milicev, Z.; Burtovyy, R.; Luzinov, I.; Yushin, G. A Major Constituent of Brown Algae for Use in High-Capacity Li-Ion Batteries. *Science* **2011**, *334*, 75–79.
25. Wu, H.; Chan, G.; Choi, J. W.; Ryu, I.; Yao, Y.; McDowell, M. T.; Lee, S. W.; Jackson, A.; Yang, Y.; Hu, L. B.; *et al.* Stable Cycling of Double-Walled Silicon Nanotube Battery Anodes through Solid-Electrolyte Interphase Control. *Nat. Nanotechnol.* **2012**, *7*, 309–314.
26. Xue, X. Y.; Wang, S. H.; Guo, W. X.; Zhang, Y.; Wang, Z. L. Hybridizing Energy Conversion and Storage in a Mechanical-to-Electrochemical Process for Self-Charging Power Cell. *Nano Lett.* **2012**, *12*, 5048–5054.
27. Zhou, J.; Gu, Y. D.; Hu, Y. F.; Mai, W. J.; Yeh, P. H.; Bao, G.; Sood, A. K.; Polla, D. L.; Wang, Z. L. Gigantic Enhancement in Response and Reset Time of ZnO UV Nanosensor by Utilizing Schottky Contact and Surface Functionalization. *Appl. Phys. Lett.* **2009**, *94*, 191103.
28. Bard, A. J.; Faulkner, L. R. *Electrochemical Methods: Fundamentals and Applications*. 2nd ed; John Wiley & Sons: New York, 2001.
29. Hsueh, C. H. Modeling of Elastic Deformation of Multilayers Due to Residual Stresses and External Bending. *J. Appl. Phys.* **2002**, *91*, 9652–9656.
30. Armstrong, G.; Armstrong, A. R.; Bruce, P. G.; Reale, P.; Scrosati, B. TiO₂(B) Nanowires as an Improved Anode Material for Lithium-Ion Batteries Containing LiFePO₄ or LiNi_{0.5}Mn_{1.5}O₄ Cathodes and a Polymer Electrolyte. *Adv. Mater.* **2006**, *18*, 2597–2600.
31. Liu, S. H.; Wang, Z. Y.; Yu, C.; Wu, H. B.; Wang, G.; Dong, Q.; Qiu, J. S.; Eychmuller, A.; Lou, X. W. A Flexible TiO₂(B)-Based Battery Electrode with Superior Power Rate and Ultralong Cycle Life. *Adv. Mater.* **2013**, *25*, 3462–3467.
32. Lin, Z. –H.; Roy, P.; Shih, Z. Y.; Ou, C. M.; Chang, H. T. Synthesis of Anatase Se/Te-TiO₂ Nanorods with Dominant {100} Facets: Photocatalytic and Antibacterial Activity Induced by Visible Light. *ChemPlusChem* **2013**, *78*, 302–309.
33. Fang, H.; Wu, W. Z.; Song, J. H.; Wang, Z. L. Controlled Growth of Aligned Polymer Nanowires. *J. Phys. Chem. C* **2009**, *113*, 16571–16574.
34. McCarty, L. S.; Whitesides, G. M. Electrostatic Charging Due to Separation of Ions at Interfaces: Contact Electrification of Ionic Electrets. *Angew. Chem., Int. Ed.* **2008**, *47*, 2188–2207.
35. Baytekin, H. T.; Patashinski, A. Z.; Branicki, M.; Baytekin, B.; Soh, S.; Grzybowski, B. A. The Mosaic of Surface Charge in Contact Electrification. *Science* **2011**, *333*, 308–312.
36. Diaz, A. F.; Felix-Navarro, R. M. A Semi-Quantitative Triboelectric Series for Polymeric Materials: the Influence of Chemical Structure and Properties. *J. Electrostat.* **2004**, *62*, 277–290.